Carbohydrate Polymers 111 (2014) 753–761

Contents lists available at ScienceDirect

Carbohydrate Polymers

journal homepage: www.elsevier.com/locate/carbpol

The synthesis, self-assembling, and biocompatibility of a novel *O*-carboxymethyl chitosan cholate decorated with glycyrrhetinic acid

Hongliang Du, Xiaoye Yang, Xin Pang, Guangxi Zhai *

Department of Pharmaceutics, College of Pharmacy, Shandong University, 44 Wenhua Xilu, Jinan 250012, China

ARTICLE INFO

Article history:
Received 10 February 2014
Received in revised form 27 April 2014
Accepted 28 April 2014
Available online 5 May 2014

Keywords:
O-carboxymethylated chitosan
Cholic acid
Glycyrrhetinic acid
Self-aggregates

ABSTRACT

O-carboxymethyl chitosan (OCMC) was firstly decorated with cholic acid (CA) to acquire an amphiphilic polymer under alkaline condition. Then glycyrrhetinic acid (GA) was conjugated to the polymer via a succinate linker and finally treated with $NaCO_3$ solution to obtain new conjugates for potential liver targeted delivery. These conjugates formed uniform aggregates with low critical aggregation concentrations (0.028–0.079 mg/mL) in PBS. The average diameter of cholic acid modified carboxymethyl chitosan (CMCA) aggregates (110–257 nm) decreased with the increase of CA substitution degree and became slightly larger after GA modification. Negative zeta potential (−15 mV) of GA decorated CMCA (GA-CMCA) revealed that the formation of negatively charged shells and spherical morphology was observed under transmission electron microscopy. Furthermore, hemolysis test, in vitro cytotoxicity assay and cellular uptake study all demonstrated the safety and feasibility of these conjugates as a promising carrier for liver targeted drug delivery.

1. Introduction

Self-aggregates developed from amphiphilic polymers have received considerable interest due to their potential pharmaceutical applications (Hoskins, Thoo-Lin, & Cheng, 2012). Such a self-assembly system consists of a hydrophobic inner core that can serve as a cargo space for hydrophobic agents and a hydrophilic outer shell that provide repulsive forces to stabilize the aggregates without any additional stabilizers (Qu et al., 2008). Also, the hydrophilic shells of these aggregates can help them avoid the uptake of the reticuloendothelial system and preferentially accumulate in target sites via the enhanced permeability and retention effect (Beck, Ourique, Guterres, & Pohlmann, 2012). Hence, polymeric self-aggregates become a promising candidate as drug carrier, which may improve the therapeutic outcome and reduce the potential toxicity of active compounds. In the past few decades, many efforts have been devoted to exploit amphiphilic polymers such as amphiphilic block copolymers (Letchford & Burt, 2007) and hydrophobically modified water-soluble polymers (Hsiao et al., 2012), which could form compact core-shell structure in an aqueous environment accompanied with self-assembly process. Recently, utilizing natural polysaccharides as water-soluble polymers such as chitosan (Cai & Jiang, 2009), dextran (Xiong, Qi, & Yao, 2012) and hyaluronan (Pravata et al., 2008) has gained increasing attention in the construction of amphiphilic polymers. In particular, self-aggregates of hydrophobically modified hydrophilic chitosan polymers are formed in aqueous media, serving as a promising carrier for transport of various active compounds.

Chitosan, the partially acetylated cationic (1-4)-2-amino-2-deoxy-β-D-glucan, is industrially produced from marine chitin. It has been used extensively as a drug carrier owing to its excellent biocompatibility and biodegradability (Busilacchi, Gigante, Mattioli-Belmonte, Manzotti, & Muzzarelli, 2013; Muzzarelli, 2009, 2010; Patel, Patel, & Patel, 2010). However, native chitosan is insoluble under physiological pH condition, which is an obstacle for its further pharmaceutical application. To solve this problem, various water-soluble chitosan derivatives such as quaternized chitosan, glycol chitosan, sulfated chitosan and carboxymethyl chitosan have been exploited successfully (Kumar, Muzzarelli, Muzzarelli, Sashiwa, & Domb, 2004). *O*-carboxymethyl chitosan is an important water-soluble derivative with improved physical and biological properties. To fabricate self-assemble system, many hydrophobic molecules such as deoxycholic acid (Jin et al., 2012), *n*-caprylic acid (Niu et al., 2013), oleic acid (Liu et al., 2013) and stearic acid (Sahu, Maiti, Maiti, Ghosh, & Pramanik, 2011) have been conjugated to the backbone of OCMC and exhibited promising application as drug carrier. CA, a main component of bile acid, possesses hydrophobic nucleus in its molecule and is often used as hydrophobic segments in chitosan based amphiphilic polymer synthesis. In recent years, cholic acid–chitosan-*g*-mPEG (Ngawhirunpat et al., 2009), glycol

* Corresponding author. Tel.: +86 531 88382015; fax: +86 531 88382731.
E-mail address: professorgxzhai@aliyun.com (G. Zhai).

http://dx.doi.org/10.1016/j.carbpol.2014.04.095
0144-8617/

chitosan–cholic acid (Hwang, Kim, Kwon, & Kim, 2008) and *N*-(2,3-dihydroxypropyl)-chitosan–cholic acid (Pan et al., 2013) have been synthesized so as to deliver various drugs. Therefore, we hypothesized that the introduction of CA onto OCMC backbone would induce self-association to form self-aggregates.

Although these self-aggregates had long circulation half-lives in bloodstream, they had to suffer from inadequate uptake by target cells and decrease the administered drug efficacy due to their non-specific property (Bertrand, Wu, Xu, Kamaly, & Farokhzad, 2014). To achieve active targeted drug delivery, molecular recognition can be utilized by conjugation of targeting molecules onto drug carriers (Du, Cai, & Zhai, 2013). GA, the hydrolysis product of glycyrrhizin, has various pharmacological activities, such as anti-inflammatory, anticancer, and antiviral effects (Lallemand et al., 2011). Recent interesting study showed GA could reverse the multidrug resistance to anticancer agents and enhance their anticancer efficiency (Nabekura, Yamaki, Ueno, & Kitagawa, 2008). Furthermore, GA was also appealing as a liver targeting ligand which could bind to specific receptors on hepatocytes, resulting receptor-mediated internalization (Cheng et al., 2013). So far, many researches indicated that drug carriers modified with GA could obviously enhance the targeting efficiency for liver targeted drug delivery than those without GA modification (Zhang, Yao, Zhou, Wang, & Zhang, 2013).

In this study, we prepared a novel amphiphilic polymer based on GA modified *O*-carboxymethyl chitosan cholate, which was synthesized by initial modification with CA to impart the polymer with hydrophobicity, followed by conjugation of GA acting as targeting ligands through a succinate linker. CMCA and GA-CMCA self-aggregates were prepared based on self-assembly and their physicochemical characteristics were studied in details. The influences of CA and GA substitution degree on the physicochemical properties have also been discussed. To understand the safety of self-aggregates after intravenous administration, the hemolytic toxicity test was investigated. Furthermore, the in vitro cytotoxicity and cellular uptake of CMCA and GA-CMCA conjugates were evaluated comparatively in HepG2 and non-liver cells.

2. Material and methods

2.1. Materials

OCMC (*Mw* = 156 kDa, *Mw*/*Mn* = 1.376, degree of deacetylation = 90%, degree of carboxymethylation = 82%) was purchased from Aoxing Biotechnology Co., Ltd. (Zhejiang, China). GA was obtained from Zelang Pharmaceutical Co. (Nanjing, China). CA, 1-ethyl-3-(3-dimethylaminopropyl)-carbodiimide hydrochloride (EDC), *N*-hydroxy succinimide (NHS), 4-dimethylaminopyridine (DMAP), *N*,*N*,*N*′,*N*′-tetramethylethylenediamine (TEMED) and pyrene were supplied by Sigma-Aldrich (USA). Sulforhodamine B (SRB), trichloroacetic acid (TCA) and Rhodamine B were purchased from Sangon Biotechnology Co. (Shanghai, China). All reagents were of analytical grade and used without further purification.

2.2. Synthesis of CMCA

OCMC was degraded using hydrochloric acid degradation method (Park et al., 2008). Briefly, OCMC (2 g) was dissolved in 50 mL hydrochloric acid (4 M), and placed in water bath at 50 °C, After incubation for a certain time, NaOH was added to neutralize the solution and dialyzed (molecular cutoff = 14 kDa) against distilled water. Then the solution was filtered and lyophilized. The molecular weight of the degraded OCMC was determined by gel permeation chromatography measurement.

CMCA was synthesized by coupling the carboxyl group of CA with the amine group of OCMC, as shown in Fig. 1. Briefly,

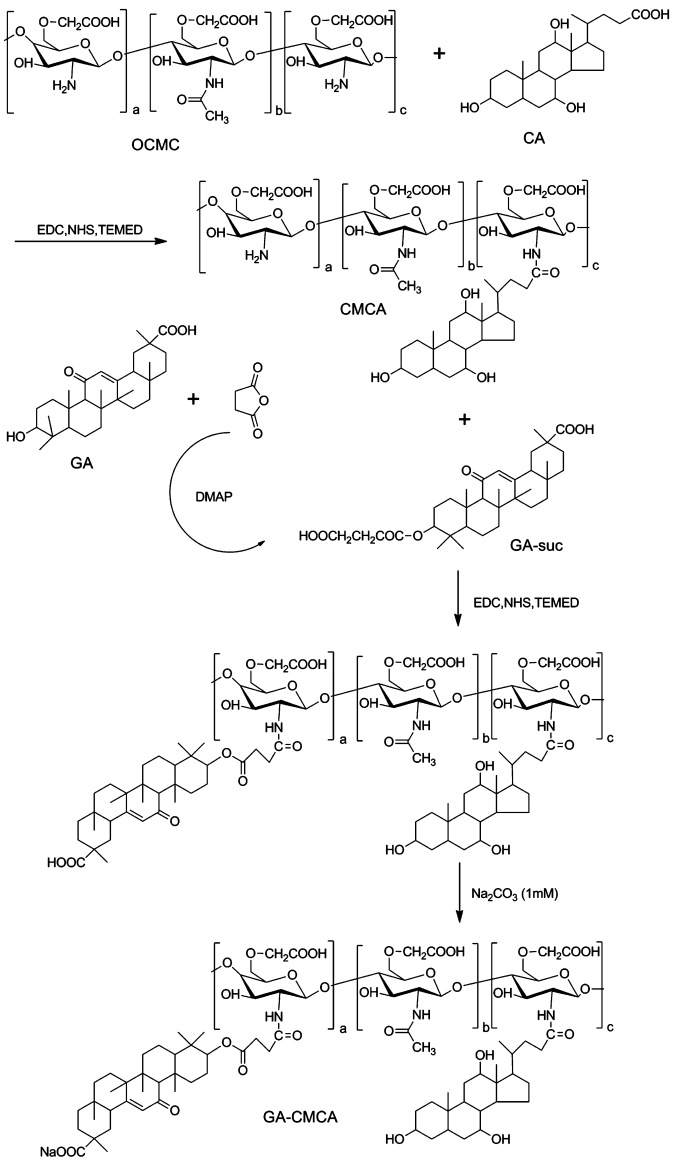

Fig. 1. Synthesis process of CMCA and GA-CMCA.

different amounts of CA (0.2–0.5 mol/mol sugar residues of OCMC) were activated by equal amounts (2 equiv./CA) of EDC and NHS at room temperature for 30 min, then TEMED (2 equiv./CA) was added and subsequent dropped into OCMC solution dissolved in distilled water and DMF (1:1, v/v). After stirring for 36 h at room temperature, the reactant mixture was dialyzed against water/methanol mixture (1:4, v/v) for 3 days and distilled water for another 3 days until no free CA was detectable in the recipient solution. The polymer was isolated by lyophilization.

2.3. Synthesis of GA-CMCA

GA-CMCA was synthesized via two steps. First, 3-*O*-hemisuccinate GA (suc-GA) was synthesized. GA (5.0 mmol), succinic anhydride (20.0 mmol) and DMAP (1 mmol) were dissolved in 50 mL anhydrous tetrahydrofuran. After reacted for 24 h at room temperature, the mixture was evaporated and further purified in a silica gel column (eluted in an ethanol-ethyl acetate (11:3; v/v) solvent system) to get suc-GA.

To activate the carboxylic acid groups of suc-GA in DMF, equal amounts (2 equiv./suc-GA) of EDC and NHS were added into the

solution and allowed for 4 h at room temperature to afford the NHS ester form of suc-GA. Then TEMED (2 equiv./CA) was added and subsequent dropped into CMCA solution dissolved in the mixture of DMF:H_2O (3:1). After stirring for 36 h at room temperature, the reaction mixture was dialyzed against water/methanol mixture (1:4) for 3 days and then against distilled water for another 3 days using a dialysis tube. To obtain the sodium salt of GA modified CMCA, the GA-CMCA solution was further dialyzed against $NaCO_3$ solution (1 mM) for 3 days and lyophilized to obtain GA-CMCA conjugates.

2.4. Structure characterization of CMCA and GA-CMCA

The chemical structures of the CMCA and GA-CMCA were confirmed by FTIR (KBr plate, Nicolet 6700 spectrometer, USA) and ^{1}H NMR (AvanceTM DPX-300, Bruker BioSpin GmbH, Rhe-instetten, Germany).

2.5. Measurement of degree of substitution

2.5.1. CA content

The molar ratios of CA to amino groups in CMCA were determined by a UV/vis spectrophotometer according to previous literatures (Yuan, Li, Zhu, & Woo, 2006). Briefly, accurately weighed CMCA was dissolved in 0.5 mL DMSO, then 0.5 mL aqueous acetic acid and 9.0 mL water/sulfuric acid (65/50, v/v) mixture were added. After homogenized, the mixture was reacted at 70 °C for 15 min. The UV absorbance at 387 nm was measured against a blank containing the same components as the sample without the polymer. The degree of substitution (DS, mol%) was calculated according to the following equation:

$$\mathrm{DS} = \left(\frac{m_1 / M_{\mathrm{CA}}}{(m - m_1) / M_{\mathrm{OCMC}}} \right)$$

where m_1 is the amount of the CA in CMCA polymer; m is the amount of the CMCA; M_{CA} is the molecular weight of the CA residue; M_{OCMC} is the molecular weight of the OCMC units.

2.5.2. GA content

The amount of GA covalently bounded to final conjugates was determined by a UV/vis spectrophotometer at λ = 250 nm. Briefly, accurately weighed GA-CMCA polymer was dissolved in water and DMSO (1/1, v/v) to obtain 0.05% polymer solution and then measured with UV/vis spectrophotometer. To acquire the calibration curve of GA-suc in the range of 5–30 μg/mL, GA-suc standard solutions with a series of gradient concentration were used. The DS (mol%) of GA to OCMC was calculated according to the following equation:

$$\mathrm{DS} = \left(\frac{m_2 / M_{\mathrm{GA\text{-}suc}}}{(m - m_1 - m_2) / M_{\mathrm{OCMC}}} \right)$$

where m_2 is the amount of the GA in GA-CMCA polymer; m_1 is the content of CA contained in the modified polymers. m is the amount of the CMCA; $M_{GA\text{-}suc}$ is the molecular weight of the GA-suc residue; M_{OCMC} is the molecular weight of the OCMC units.

2.6. Preparation of self-assembled nanoparticles

CMCA and GA-CMCA conjugates were suspended in PBS (pH 7.4) at the concentration of 1 mg/mL under gentle shaking at room temperature for overnight. Then, the solution was sonicated with a probe sonicator at 120 W for 2 min. The sonication pulse was turned on 2 s with an interval of 4 s. Finally, the solutions were filtered with 0.45 μm syringe filter and stored at 4 °C.

The size and zeta potential of the aggregates were determined by Delsa™ Nano Submicron Particle Size Analyzer (Beckman Counter Co., Ltd, USA). All samples were tested in triplicate. The morphology of self-assembles was observed using JEM-100CX II transmission electron microscope (TEM).

2.7. Critical aggregation concentration of conjugates

The self-aggregation behaviors of conjugates in PBS 7.4 were estimated by fluorescence spectroscopy using pyrene as hydrophobic fluorescence probe (Guo et al., 2013). Briefly, the pyrene solutions (6.0×10^{-5} M) in acetone were added into the tubes and evaporated to dryness under a stream of nitrogen gas. A serial of CMCA and GA-CMCA solutions with concentrations ranging from 1×10^{-3} to 0.5 mg/mL were added to each tube with a constant pyrene concentration of 6.0×10^{-7} M. Then the solutions were sonicated in an ultrasonic bath for 40 min and left undisturbed to equilibrate for 8 h at 37 °C. Fluorescence spectra of pyrene were recorded with a F-7000 spectrophotometer (Hitachi, Japan) at room temperature. The slit widths for excitation and emission were set at 5.0 and 2.5 nm, respectively. The emission spectra of pyrene were performed at a range from 350 to 500 nm at the excitation wavelength of 334 nm.

2.8. Hemolytic test

Two percent erythrocytes suspension was acquired using freshly rabbit blood. Each 2.5 mL erythrocytes suspension was mixed with different aggregates and the total volume was kept in 5 mL. All the suspensions were incubated at 37 °C for 1 h and then centrifuged at 4000 rpm for 10 min to remove the intact erythrocytes. Subsequently, the absorbance of supernatants was measured spectrophotometrically at 541 nm which was the typical absorbance of hemoglobin. Deionized water as positive control was mixed with the erythrocytes suspension, while saline solution was used in experiments for negative control. The degree of hemolysis was determined using the following equation:

$$\text{Percentage of hemolysis} = \left(\frac{A_{\mathrm{sample}} - A_{\mathrm{negative}}}{A_{\mathrm{positive}} - A_{\mathrm{negative}}} \right)$$

where A_{sample}, $A_{negative}$, $A_{positive}$ refer to the absorption of samples used in experiments, negative control and positive control at 541 nm, respectively.

2.9. In vitro cytotoxicity assay of self-aggregates

The in vitro cytotoxicity of CMCA and GA-CMCA self-aggregates were evaluated in Hela and HepG2 cell lines by sulforhodamine B Dye (SRB Assay) (Kumar, Chashoo, Saxena, & Pandey, 2013). Briefly, Hela and HepG2 cells in their logarithmic growth were seeded in 96-well plates at a seeding density of 5000 cells/well/100 μL DMEM medium, respectively. Following incubation overnight, the culture medium was carefully replaced with 100 μL of medium containing serial dilutions of CMCA and GA2-CMCA self-aggregates. The concentrations of the aggregates used in the experiments were ranging from 0.01 to 0.5 mg/mL. Cells were incubated with treatments for 72 h and then the cells viability was determined. In detail, the cell growth was arrested by layering 50 μL of 50% TCA and incubated at 4 °C for 1 h. After washing and drying the plate, SRB (100 μL, 0.4% in 1% acetic acid) was added at room temperature and kept for 30 min. 1% acetic acid was used to wash the unbound SRB dye and air dried. Then Tris–HCl bufer (100 μL, 0.01 M, pH 10.4) was added and the absorbance of each well was read on a microplate reader (Bio-Rad 680, USA) at a test wavelength of 570 nm. All the experiments were done with 10 parallel samples. Suitable blanks

and positive controls were also included. The percentage of cell viability rate was calculated as follows:

$$\text{Percentage of hemolysis} = \left(\frac{A_{\text{sample}} - A_{\text{negative}}}{A_{\text{positive}} - A_{\text{negative}}}\right)$$

2.10. In vitro cellular uptake

In order to investigate the potential liver targeting ability of GA-CMCA, the cellular uptake study was conducted against different human cancer cell lines: MCF-7 cells (breast cancer), Hela cells (cervical cancer) and HepG2 cells (liver cancer). For fluorescence microscopy observation, all experimental cells in their logarithmic growth were cultured for 24 h for attachment, and then were washed with PBS three times. Aliquots cell suspensions were incubated with free rhodamine B (free R-B), CMCA rhodamine B (CMCA/R-B) and GA-CMCA rhodamine B (GA-CMCA/R-B) at a final R-B concentration of 5 μM for 2 h at 37 °C. After incubation, the cells were washed three times with precooled PBS to remove unbound R-B. An aliquot of cells was taken to be examined on a fluorescence microscope and photographed.

3. Results and discussion

3.1. Synthesis and characterization of conjugates

The molecule weight of OCMC is a key factor influencing the synthesis and construction of nanosized self-aggregates. In the study, we prepared three types of OCMC with different molecular weights by acidic degradation. After incubation of commercial OCMC in acidic conditions for 2 h and 6 h, the molecular weights (*Mw*) of the material were 52 kDa and 17 kDa with molecular weight distribution (*Mw*/*Mn*) of 1.449 and 1.475, respectively. By controlling the molar ratio of cholic acid to OCMC sugar residues at 4:10, CMCA conjugates with different degree of substitution were obtained due to the difference of molecular weights, which was dissimilar to previous literatures (Park et al., 2007). High viscosity property of high molecules weight OCMC in reaction solution could reduce the reactive activity of primary amines on the backbone, therefore with the increase of OCMC molecules weight from 17 kDa to 156 kDa, the DS decreased from 11.8% to 7.9%. Self-assembled aggregates of CMCA conjugates were prepared by simple sonication in aqueous environment. The size of CMCA aggregates increased slightly from 120 nm to 189 nm and further to 257 nm with the increase of molecular weight. To obtain self-aggregates with high DS and appropriate size, OCMC with 17 kDa molecular weight was chosen as the original polymer in the subsequent study.

As shown in Fig. 1, CA and GA-suc were covalently linked to primary amine group of the OCMC in the presence of EDC and NHS. To avoid the possible precipitatation of OCMC polymer due to the decrease of pH, TEMED as an acid-binding agent was added before the reaction. The ^{1}H NMR spectra of GA, GA-suc, OCMC, CMCA, GA-CMCA were depicted in Fig. 2. Compared to the spectrum of GA, the signals of GA-suc around 3.0 ppm were transferred to 4.4 ppm which could confirm the change of chemical environment of carbon proton at —OH group after succinic anhydride conjugation. New peaks appeared around at 2.4 ppm were attributed to $-CH_2$ protons of succinic anhydride. For quantitative analysis, the amount of —COOH was doubled according to the peak area ratio at 12.18 ppm and 5.40 ppm. Mass spectrum confirmed the molecular weight of GA-suc was increased from 469.6 to 569.6 Da after conjugation. For OCMC, typical peak at 2.0 ppm was assigned to the methyl hydrogen of *N*-acetylglucosamine. The ring protons of OCMC showed apparent broad peaks at 3.4–4.0 ppm. In the spectrum of CMCA, new peaks at 0.6–2.5 ppm were ascribed to the ring protons of CA, indicating the presence of CA moieties in CMCA. While for GA-CMCA, the new proton peak at 5.73 ppm was the characteristic peak of GA. Moreover, the signals ranging of 0.6–1.6 ppm which were considered as the peaks of ring protons of GA were overlapped with the CA peaks, thus the signals in these positions were enhanced significantly.

Successful synthesis of CMCA and GA-CMCA polymer was also confirmed by FT-IR spectrum (data not shown). The characteristic strong absorption bands of OCMC at 1602 cm^{-1} was ascribed to the N—H bending vibration of abundant primary amines, which covered the amide I and II band of amide, indicating the high degree of deacetylation of OCMC (Wang et al., 2011). For the CMCA spectrum, dramatic decrease of the absorption band of N—H bending vibration was observed while the amide I band stretching vibration at slightly higher wavenumbers was strengthened, revealing formation of amide linkages. In comparison with CMCA, the amide II band of GA-CMCA further decreased along with the increase of amide I band signal. Furthermore, the amide III band at 1385 cm^{-1} was evidently strengthened after conjugation of CA and GA onto OCMC backbone by acylation of amide linkages.

By controlling the feed ratio of CA and OCMC in the coupling reaction, various CMCA polymers with different DS were prepared. Results were shown in Table 1. The DS of the CA varied from 4.0% to 12.7% with the feed ratio increased from 2:10 to 5:10. In this experiment, the degree of deacetylation of OCMC was 90%, when the feed ratio of CA and OCMC increased from 4:10 to 5:10, no conspicuous increase (from 11.8% to 12.7%) of DS was observed. That is to say, many free amino groups could not further react with more CA after a certain amount of CA conjugation. To obtain more active primary amines for GA-suc coupling, CMCA2 with 8.2% DS and 3:10 feed ratio was chosen as the intermediate polymer in the further study. For GA-CMCA, the GA substitution degree could up to 6.5% measured by the UV spectroscopy method as described in Section 2.

3.2. Self-aggregation of CMCA and GA-CMCA

CMCA and GA-CMCA conjugates, composed of the hydrophilic polymer OCMC and hydrophobic cholic acid segment, could self-assemble in aqueous solution due to several forces, such as the hydrophobic effect of CA, the hydrogen bonding among hydrophilic segments, and the hydrogen bonding of hydrophilic segments and water molecules. These forces also influenced the size and morphology of the aggregates as well as inducing the self-aggregation of amphiphilic polymer (Lee, Huang, &, Lee, 2006). Moreover, the self-assembly process did not need any additives and could be promoted by ultrasonic. GA, as a targeting molecule, could be dissolved in the PBS medium (pH 7.4) after handled with Na_2CO_3 (1 mM) during the conjugates synthesis and presented on the surface of the nano-aggregates.

The particle size and size distribution of CMCA and GA-CMCA aggregates with different DS in PBS solution (pH = 7.4) were measured by Size Analyzer. As depicted in Table 1, the average sizes of CMCA aggregates were in the range of 110–254 nm with relatively narrow size distribution (0.073–0.242). With the increase of cholic acid DS, the particle size decreased. It could be attributed to the enhanced hydrophobic interaction between hydrophobic segments and more tightly packed hydrophobic cores were formed when more CA were conjugated to OCMC. Using CMCA2 in further GA coupling reaction, GA-CMCA were obtained and showed slightly larger particle size than those of CMCA aggregates, which indicated that most of the GA-suc residues could be dissolved in the PBS media as its sodium salt and had little hydrophobicity in the self-assembly solution, resulting more soluble of conjugates (Guo et al., 2013). This phenomenon revealed that GA as targeting molecules could present on the surface of self-aggregates.

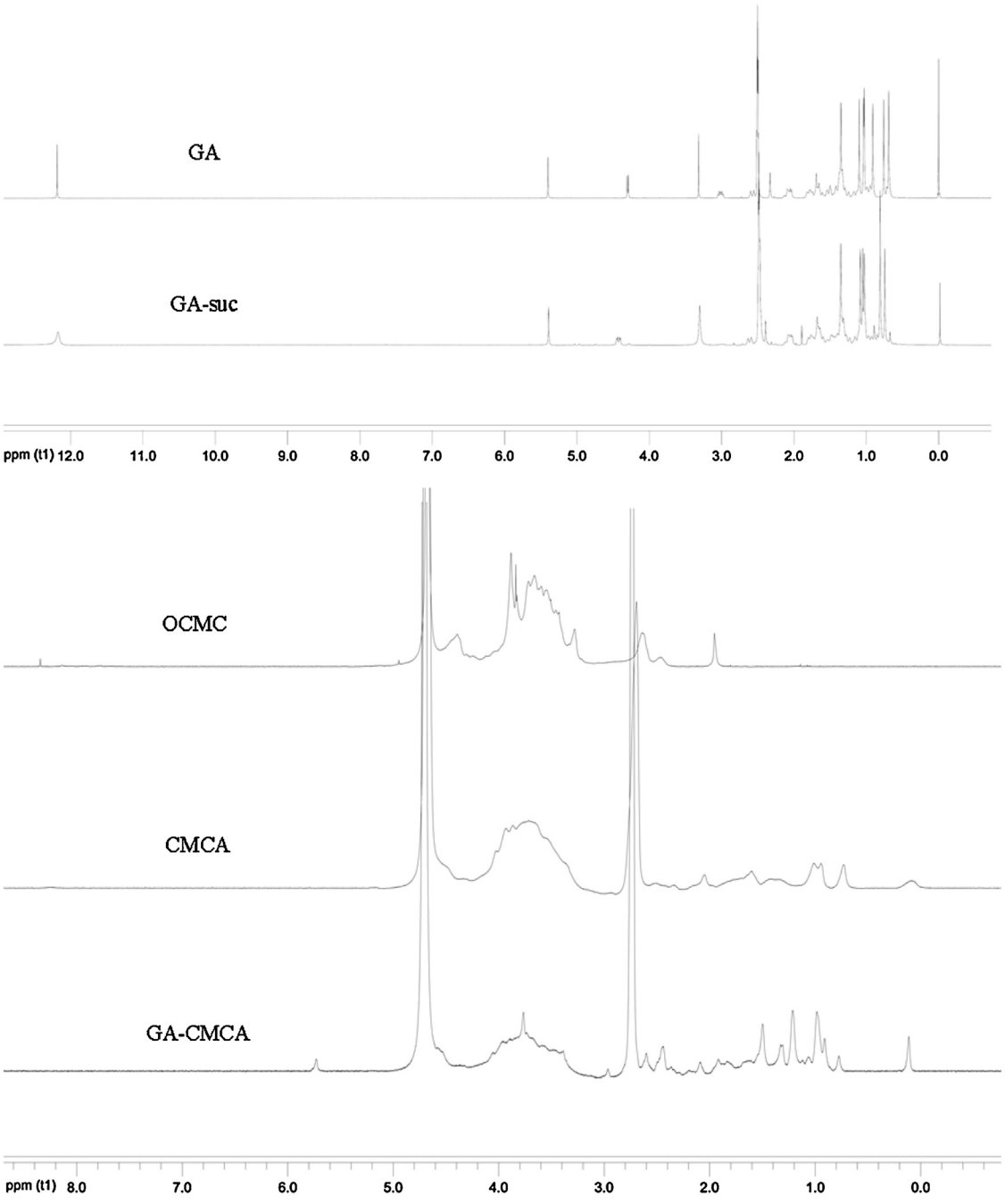

Fig. 2. The ^{1}H NMR spectra of GA and GA-suc in DMSO-d6, OCMC in D_2O, CMCA and GA-CMCA in D_2O/DMSO-d6 (1:1, v/v) at 25 °C.

This deduction will be further confirmed in our future study. TEM observation demonstrated the formation of self-aggregates with spherical morphology. As shown in Fig. 3, the spherical particles with a uniform size distribution could disperse well without any aggregation. However, the average diameter of self-aggregates observed by TEM method was smaller than that by Size Analyzer. Similar findings revealed that the drying procedure of TEM sample preparation could contribute to the size difference (Jiang, Quan, Liao, & Wang, 2006). Zeta potentials of CMCA and GA-CMCA self-aggregates were around −17 mV and −15 mV, respectively, which

Table 1
Properties of CMCA and GA-CMCA conjugates in PBS solution (pH 7.4).

Sample	DS (%)	Diameter (nm)	Polydispersity index	Zeta potential (mV)	CAC (mg/mL)
CMCA1	4.0	253.6 ± 4.91	0.126 ± 0.031	−18.62 ± 0.85	0.079
CMCA2	8.2	181.7 ± 4.64	0.073 ± 0.027	−17.11 ± 0.73	0.046
CMCA3	11.8	120.1 ± 6.81	0.193 ± 0.051	−16.32 ± 1.24	0.034
CMCA4	12.7	110.0 ± 6.52	0.242 ± 0.020	−16.21 ± 1.02	0.028
GA1-CMCA2	4.1	190.7 ± 8.94	0.159 ± 0.039	−15.48 ± 0.49	0.054
GA2-CMCA2	6.5	193.9 ± 7.63	0.213 ± 0.091	−14.97 ± 1.33	0.067

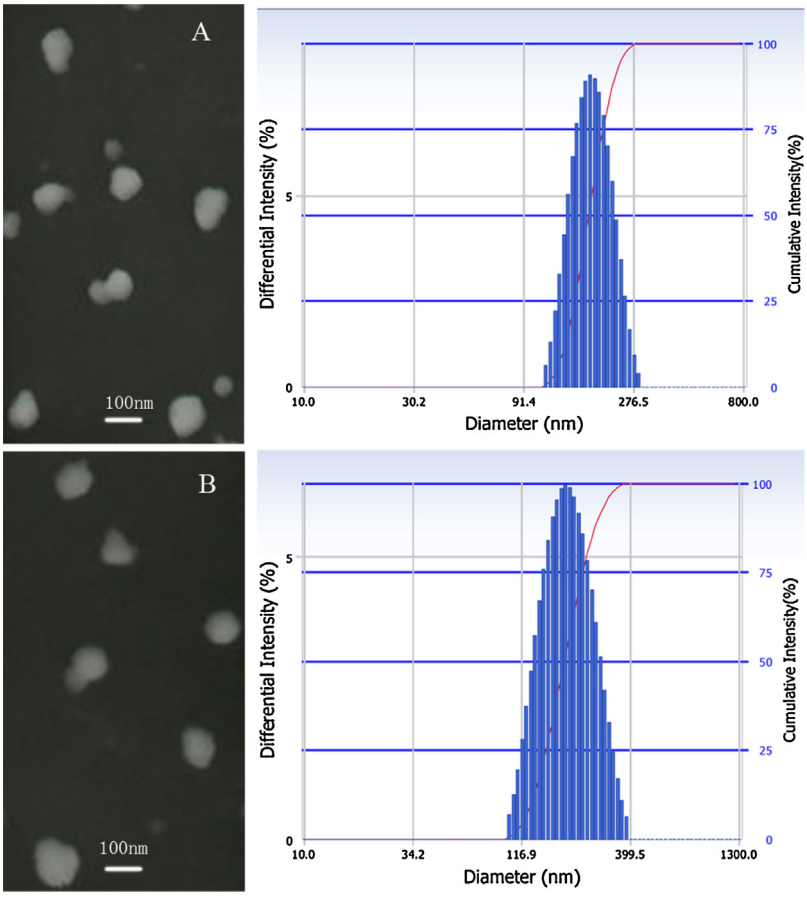

Fig. 3. The TEM images of CMCA (A) and GA-CMCA (B) self-aggregates.

revealed that the surfaces of the nano-aggregates were covered with hydrophilic negatively charged carboxymethyl groups, proving the formation of self-aggregates system. Besides, CMCA and GA-CMCA self-aggregates all exhibited satisfactory stability without any precipitation for over 1 month at 4 °C. The tight interaction of hydrophobic cores and blocking effect of hydrophilic shells contributed to the stability of self-aggregates.

3.3. Critical aggregation concentration of conjugates

The fluorescence probe technique was performed to investigate the aggregation behavior of CMCA and GA-CMCA conjugates. Pyrene molecules as probe could exhibit different photophysical characteristics according to the changes of solution polarity. When self-aggregates were formed in aqueous solution, pyrene molecules preferred to locate inside or close to hydrophobic cores of aggregates, resulting the alteration of fluorescence properties. Generally, five vibrational peaks can be observed in the pyrene emission spectra. The intensity ratio of the first peak (373 nm) and the third peak (384 nm) I_1/I_3 is fairly sensitive to the polarity of the microenvironment and can be used to establish the interrelationship with the concentration of amphiphilic polymer (Hu, Li, Yuan, & Zeng, 2006). When amphiphilic polymer is at low concentration, the value of ratio keeps fairly constant or changes slightly. However, when the concentration exceeds a certain level, dramatic decline of the ratio occurs along with the drastic increases of the intensity of the third highest vibrational band at 384 nm. This concentration is defined as critical aggregation concentration (CAC), meaning the threshold concentration of polymer aggregates formation. Obviously, lower CAC value indicates that self-aggregates can form at relatively low concentration and have better stability of aggregates under similar diluted conditions.

The CAC curves of CMCA2 and GA2-CMCA2 determined from emission spectra of pyrene in PBS (pH 7.4) solutions were shown in Fig. 4. The CAC values of the CMCA conjugates were in the range of 0.028–0.079 mg/mL, which declined with the increase of CA substitution degree (Table 2). The CAC values of these conjugates were much lower than those of low molecular weight surfactants, such as SDS with CAC of 2.3 mg/mL (Rahman & Brown, 1983), revealing that a novel kind of amphiphilic polymers was developed. As for GA-CMCA, the CAC values were slightly higher than that of CMCA conjugates with same DS of CA, which illustrated that most of GA were not involved in the hydrophobic interaction in the media but on the surface of self-aggregates as hydrophilic targeting molecules. These results were consistent with former particle size study.

3.4. Hemolytic test

In order to evaluate the potential use of self-aggregates in injectable drug formulations, the hemolytic toxicity of different

Table 2
Results of hemolytic toxicity study of CMCA ang GA-CMCA conjugates.

Sample	Concentration (mg/mL)		
	1	2	3
CMCA1	0.029 ± 0.012	0.047 ± 0.008	0.062 ± 0.026
CMCA2	5.9 ± 1.5	38.6 ± 5.1	50.9 ± 4.6
CMCA3	17.2 ± 4.8	54.4 ± 8.3	63.9 ± 6.2
GA2-CMCA2	0.097 ± 0.041	0.76 ± 0.21	4.4 ± 2.2

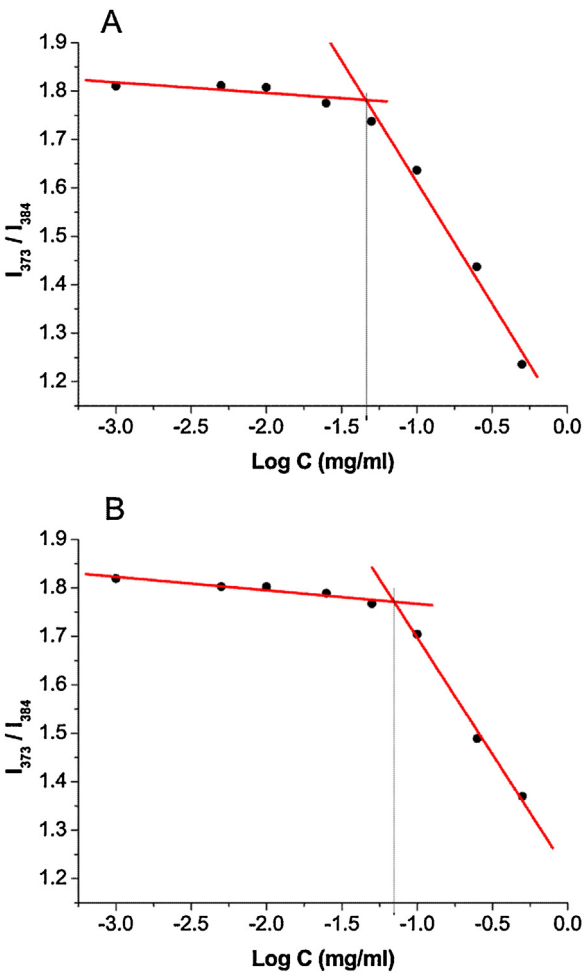

Fig. 4. Plot of the intensities ratio (I_{373}/I_{384}) from pyrene excitation spectra as a function of the logarithms of concentration of CMCA (A) and GA-CMCA (B) self-aggregates in PBS solution (pH 7.4) at room temperature.

conjugates was examined. The results of a series of aggregates with different concentration after 1 h incubation were illustrated in Table 1. Overall, the hemolytic toxicity rapidly increased with the increase of polymer concentration. For CMCA2 aggregates, the hemolysis percents increased from 5.9% to 50.9% when the polymer concentration increased from 1 to 3 mg/mL. Interestingly, CMCA1 with lower CA substitution degree showed little hemolytic toxicity to blood cells while higher hemolytic toxicity was observed for CMCA3 in comparison with those for CMCA2. The possible reason for this was that as increasing DS of CA should present CA on the surface of self-aggregates, which could interact with blood cell components, resulting in increasingly hemolysis. However, after conjugation of GA-suc to CMCA2, dramatic decreases of hemolysis ratios were observed. To some extent, this result also revealed that GA could dissolve in aqueous solution as a portion of hydrophilic shells and isolate the hydrophobic cores. Except for CMCA2 and CMCA3, the hemolytic ratios of all other self-aggregates were less than 5%, indicating their good safety in blood-contacting application.

3.5. *In vitro cytotoxicity assay and cellular uptake*

The cytotoxicity of CMCA and GA-CMCA self-aggregates was tested against Hela and HepG2 cell lines at the concentration from 0.01 to 0.5 mg/mL using SRB assay (Fig. 5). The CMCA self-aggregates almost did not show any cytotoxicity to Hela and HepG2 cells at all experimental concentrations which could be considered as a safe carrier for biomedical applications. While for GA-CMCA aggregates, considerable decline of cell viability (4.1% survival rate for Hela cells and 13.6% for HepG2 cells) was observed at high polymer concentration (0.5 mg/mL) though insignificant cytotoxicity was shown below concentration of 0.25 mg/mL. This phenomenon was probably ascribed to the nature of GA. GA, which was used as a liver targeting molecule, was also an important active compound, which had been reported to possess in vitro growth inhibiting activity to mouse and human cancer cell lines (Yadav et al., 2014). The free GA could free from the polymer backbone after internalized by experimental cells, resulting cytotoxicity. Therefore, when the concentration of GA-CMCA aggregates was lower than 0.25 mg/mL, the polymer could be used as a safe carrier for drug delivery and the incorporated GA acted as potential liver targeting molecules. Interestingly, the polymer itself could be considered as a hydrophilic active agent as well at higher concentrations (>0.5 mg/mL).

To visualize the drug delivery profiles of self-aggregates, rhodamine B was loaded into the self-aggregates and applied to cellular uptake by HepG2 cells and non-liver cells. As shown in Fig. 6, cellular uptake of free R-B was similar in all experimental cells and relatively weak fluorescence intensity could be observed under fluorescence microscopy. However, formulated rhodamine B showed significant increase of cellular uptake with all experimental cells after 2 h incubation. Especially for HepG2 cells, GA-CMCA aggregates had a marked increase in cellular uptake compared to CMCA aggregates, indicating its potential targeted ability to liver cells. As for MCF-7 and Hela cells, there was no obvious difference in the

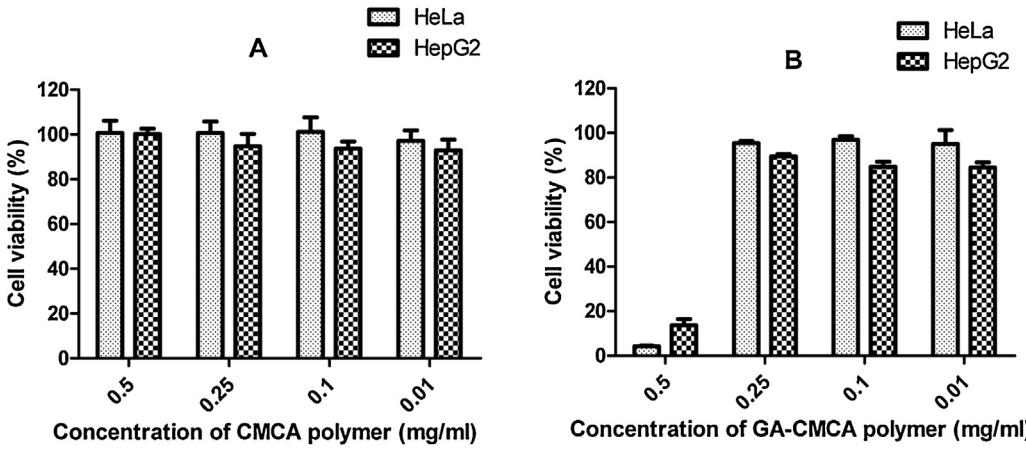

Fig. 5. Cytotoxicity of CMCA (A) and GA-CMCA (B) self-aggregates using SRB assay.

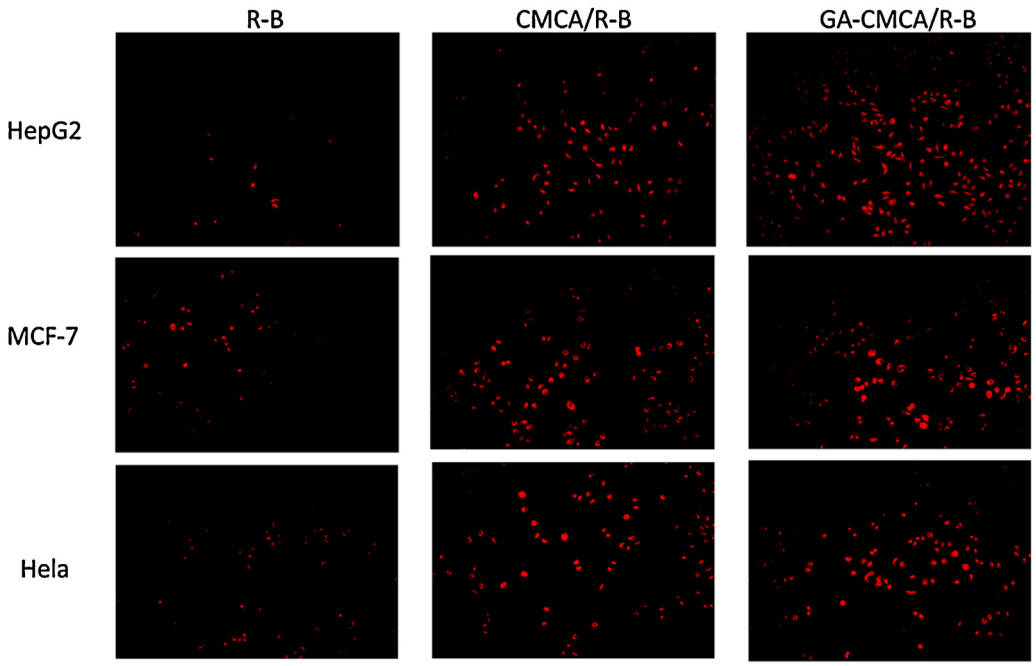

Fig. 6. Uptake of free rhodamine B (R-B), R-B-loaded CMCA (CMCA/R-B), and R-B-loaded GA-CMCA(GA-CMCA/R-B) in HepG2, MCF-7 and Hela cells after 2 h incubation.

cellular uptake between the CMCA aggregates and GA-CMCA aggregates, suggested the specific GA receptor mediated internalization may be involved in the cellular uptake by HepG2 cells while no or less GA receptor was presented on MCF-7 and Hela cells surfaces.

4. Conclusions

In the present study, novel amphiphilic chitosan derivatives, namely, CMCA and GA-CMCA conjugates, were synthesized as potential drug delivery systems. CMCA conjugates could self-assemble into stable self-aggregates in aqueous media with mean diameter of 110–254 nm and became slightly larger after GA conjugation. The CAC of CMCA conjugates were low (0.028–0.079 mg/mL) while the values of GA-CMCA conjugates were slightly higher than those of CMCA in PBS solution (pH 7.4). Results demonstrated that in the construction of GA-CMCA self-aggregates, CA as hydrophobic domains formed compact core and most of the GA as targeting molecules were in sodium salt form and presented on the surfaces of aggregates. The hemolysis test demonstrated the good compatibility of GA-CMCA with blood cells and could be safely used as excipient for injectable drug formulations. The GA decorated polymer showed concentration dependent cytotoxicity in vitro, which could be considered as a safe carrier for targeted drug delivery when the aggregates concentration was below 0.25 mg/mL. Furthermore, GA-CMCA conjugates have the ability to target specifically the liver cancer cells, which may enhance the therapeutic efficiency of drugs with less damage to other tissues. These results suggested the potential applicability of GA-CMCA self-aggregates and provide essential physicochemical and biological parameters for their further pharmaceutical investigations.

Acknowledgment

Financial support from the Natural Science Foundation of Shandong Province, China (No. ZR2011HM026) is gratefully acknowledged.

References

Beck, R. C., Ourique, A. F., Guterres, S. S., & Pohlmann, A. R. (2012). Spray-dried polymeric nanoparticles for pharmaceutics: A review of patents. *Recent Patents on Drug Delivery & Formulation*, *6*(3), 195–208.

Bertrand, N., Wu, J., Xu, X., Kamaly, N., & Farokhzad, O. C. (2014). Cancer nanotechnology: The impact of passive and active targeting in the era of modern cancer biology. *Advanced Drug Delivery Reviews*, *66*, 2–25.

Busilacchi, A., Gigante, A., Mattioli-Belmonte, M., Manzotti, S., & Muzzarelli, R. A. (2013). Chitosan stabilizes platelet growth factors and modulates stem cell differentiation toward tissue regeneration. *Carbohydrate Polymers*, *98*(1), 665–676.

Cai, G., & Jiang, H. (2009). pH-sensitive nanoparticles self-assembled from a novel class of biodegradable amphiphilic copolymers based on chitosan. *Journal of Materials Science—Materials in Electronics*, *20*(6), 1315–1320.

Cheng, M., Xu, H., Wang, Y., Chen, H., He, B., Gao, X., Li, Y., Han, J., & Zhang, Z. (2013). Glycyrrhetinic acid-modified chitosan nanoparticles enhanced the effect of 5-fluorouracil in murine liver cancer model via regulatory T-cells. *Drug Design, Development and Therapy*, *7*, 1287–1299.

Du, H., Cai, X., & Zhai, G. (2013). Advances in the targeting molecules modified chitosan-based nanoformulations. *Current Drug Targets*, *14*(9), 1034–1052.

Guo, H., Zhang, D., Li, C., Jia, L., Liu, G., Hao, L., Zheng, D., Shen, J., Li, T., Guo, Y., & Zhang, Q. (2013). Self-assembled nanoparticles based on galactosylated *O*-carboxymethyl chitosan-graft-stearic acid conjugates for delivery of doxorubicin. *International Journal of Pharmaceutics*, *458*(1), 31–38.

Hoskins, C., Thoo-Lin, P. K., & Cheng, W. P. (2012). A review on comb-shaped amphiphilic polymers for hydrophobic drug solubilization. *Therapeutic Delivery*, *3*(1), 59–79.

Hsiao, M. H., Larsson, M., Larsson, A., Evenbratt, H., Chen, Y. Y., Chen, Y. Y., & Liu, D. M. (2012). Design and characterization of a novel amphiphilic chitosan nanocapsule-based thermo-gelling biogel with sustained in vivo release of the hydrophilic anti-epilepsy drug ethosuximide. *Journal of Controlled Release*, *161*(3), 942–948.

Hu, F. Q., Li, Y. H., Yuan, H., & Zeng, S. (2006). Novel self-aggregates of chitosan oligosaccharide grafted stearic acid: Preparation, characterization and protein association. *Die Pharmazie*, *61*(3), 194–198.

Hwang, H. Y., Kim, I. S., Kwon, I. C., & Kim, Y. H. (2008). Tumor targetability and antitumor effect of docetaxel-loaded hydrophobically modified glycol chitosan nanoparticles. *Journal of Controlled Release*, *128*(1), 23–31.

Jiang, G.-B., Quan, D., Liao, K., & Wang, H. (2006). Preparation of polymeric micelles based on chitosan bearing a small amount of highly hydrophobic groups. *Carbohydrate Polymers*, *66*(4), 514–520.

Jin, Y. H., Hu, H. Y., Qiao, M. X., Zhu, J., Qi, J. W., Hu, C. J., Zhang, Q., & Chen, D. W. (2012). pH-sensitive chitosan-derived nanoparticles as doxorubicin carriers for effective anti-tumor activity: Preparation and in vitro evaluation. *Colloids and Surfaces B: Biointerfaces*, *94*, 184–191.

Kumar, M. N., Muzzarelli, R. A., Muzzarelli, C., Sashiwa, H., & Domb, A. J. (2004). Chitosan chemistry and pharmaceutical perspectives. *Chemical Reviews*, *104*(12), 6017–6084.

Kumar, S., Chashoo, G., Saxena, A. K., & Pandey, A. K. (2013). *Parthenium hysterophorus*: A probable source of anticancer, antioxidant and anti-HIV agents. *BioMed Research International*, *2013*, 810734.

Lallemand, B., Gelbcke, M., Dubois, J., Prevost, M., Jabin, I., & Kiss, R. (2011). Structure-activity relationship analyses of glycyrrhetinic acid derivatives as anticancer agents. *Mini Reviews in Medicinal Chemistry*, *11*(10), 881–887.

Lee, C. T., Huang, C. P., & Lee, Y. D. (2006). Preparation of amphiphilic poly(L-lactide)-graft-chondroitin sulfate copolymer self-aggregates and its aggregation behavior. *Biomacromolecules*, *7*(4), 1179–1186.

Letchford, K., & Burt, H. (2007). A review of the formation and classification of amphiphilic block copolymer nanoparticulate structures: Micelles, nanospheres, nanocapsules and polymersomes. *European Journal of Pharmaceutics and Biopharmaceutics*, *65*(3), 259–269.

Liu, Y., Kong, M., Feng, C., Yang, K. K., Li, Y., Su, J., Cheng, X. J., Park, H. J., & Chen, X. G. (2013). Biocompatibility, cellular uptake and biodistribution of the polymeric amphiphilic nanoparticles as oral drug carriers. *Colloids and Surfaces B: Biointerfaces*, *103*, 345–353.

Muzzarelli, R. A. (2009). Chitins and chitosans for the repair of wounded skin, nerve, cartilage and bone. *Carbohydrate Polymers*, *76*(2), 167–182.

Muzzarelli, R. A. (2010). Chitins and chitosans as immunoadjuvants and non-allergenic drug carriers. *Marine Drugs*, *8*(2), 292–312.

Nabekura, T., Yamaki, T., Ueno, K., & Kitagawa, S. (2008). Inhibition of *P*-glycoprotein and multidrug resistance protein 1 by dietary phytochemicals. *Cancer Chemotherapy and Pharmacology*, *62*(5), 867–873.

Ngawhirunpat, T., Wonglertnirant, N., Opanasopit, P., Ruktanonchai, U., Yoksan, R., Wasanasuk, K., & Chirachanchai, S. (2009). Incorporation methods for cholic acid chitosan-*g*-mPEG self-assembly micellar system containing camptothecin. *Colloids and Surfaces B: Biointerfaces*, *74*(1), 253–259.

Niu, J., Huang, A., Xiao, Y., Su, Z., Li, H., Ping, Q., Bao, X., Li, S., Chen, Y., & Sun, M. (2013). Octreotide-mediated tumor cell uptake and intracellular pH-responsive drug delivery of the self-assembly supramolecular nanocarrier. *Journal of Drug Targeting*, *21*(5), 415–426.

Pan, Z., Gao, Y., Heng, L., Liu, Y., Yao, G., Wang, Y., & Liu, Y. (2013). Amphiphilic *N*-(2,3-dihydroxypropyl)-chitosan–cholic acid micelles for paclitaxel delivery. *Carbohydrate Polymers*, *94*(1), 394–399.

Park, K., Hong, H. Y., Moon, H. J., Lee, B. H., Kim, I. S., Kwon, I. C., & Rhee, K. (2008). A new atherosclerotic lesion probe based on hydrophobically modified chitosan nanoparticles functionalized by the atherosclerotic plaque targeted peptides. *Journal of Controlled Release*, *128*(3), 217–223.

Park, K., Kim, J. H., Nam, Y. S., Lee, S., Nam, H. Y., Kim, K., Park, J. H., Kim, I. S., Choi, K., Kim, S. Y., & Kwon, I. C. (2007). Effect of polymer molecular weight on the tumor targeting characteristics of self-assembled glycol chitosan nanoparticles. *Journal of Controlled Release*, *122*(3), 305–314.

Patel, M. P., Patel, R. R., & Patel, J. K. (2010). Chitosan mediated targeted drug delivery system: A review. *Journal of Pharmacy & Pharmaceutical Sciences*, *13*(4), 536–557.

Pravata, L., Braud, C., Boustta, M., El Ghzaoui, A., Tommeraas, K., Guillaumie, F., Schwach-Abdellaoui, K., & Vert, M. (2008). New amphiphilic lactic acid oligomer–hyaluronan conjugates: Synthesis and physicochemical characterization. *Biomacromolecules*, *9*(1), 340–348.

Qu, X., Omar, L., Le, T. B., Tetley, L., Bolton, K., Chooi, K. W., Wang, W., & Uchegbu, I. F. (2008). Polymeric amphiphile branching leads to rare nanodisc shaped planar self-assemblies. *Langmuir*, *24*(18), 9997–10004.

Rahman, A., & Brown, C. (1983). Effect of pH on the critical micelle concentration of sodium dodecyl sulphate. *Journal of Applied Polymer Science*, *28*(4), 1331–1334.

Sahu, S. K., Maiti, S., Maiti, T. K., Ghosh, S. K., & Pramanik, P. (2011). Hydrophobically modified carboxymethyl chitosan nanoparticles targeted delivery of paclitaxel. *Journal of Drug Targeting*, *19*(2), 104–113.

Wang, F., Zhang, D., Duan, C., Jia, L., Feng, F., Liu, Y., Wang, Y., Hao, L., & Zhang, Q. (2011). Preparation and characterizations of a novel deoxycholic acid–*O*-carboxymethylated chitosan–folic acid conjugates and self-aggregates. *Carbohydrate Polymers*, *84*(3), 1192–1200.

Xiong, Y., Qi, J., & Yao, P. (2012). Amphiphilic cholic-acid-modified dextran sulfate and its application for the controlled delivery of superoxide dismutase. *Macromolecular Bioscience*, *12*(4), 515–524.

Yadav, D. K., Kalani, K., Singh, A. K., Khan, F., Srivastava, S. K., & Pant, A. B. (2014). Design, synthesis and in vitro evaluation of 18beta-glycyrrhetinic acid derivatives for anticancer activity against human breast cancer cell line MCF-7. *Current Medicinal Chemistry*, *21*(9), 1160–1170.

Yuan, X. B., Li, H., Zhu, X. X., & Woo, H. G. (2006). Self-aggregated nanoparticles composed of periodate-oxidized dextran and cholic acid: Preparation, stabilization and in-vitro drug release. *Journal of Chemical Technology and Biotechnology*, *81*(5), 746–754.

Zhang, L., Yao, J., Zhou, J., Wang, T., & Zhang, Q. (2013). Glycyrrhetinic acid-graft-hyaluronic acid conjugate as a carrier for synergistic targeted delivery of antitumor drugs. *International Journal of Pharmaceutics*, *441*(1-2), 654–664.